


Declaration

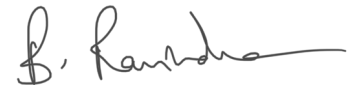
I hereby declare that the work presented in this Thesis titled "*Analysis of Lattice Boltzmann Method for Turbulent Flow Simulation on Multi-core GPU Architecture*" submitted to the Indian Institute of Technology Jodhpur in partial fulfilment of the requirements for the award of the degree of Doctor of Philosophy, is a bonafide record of the research work carried out under the joint supervision of *Dr. B.Ravindra* and *Dr. Akshay Prakash*. The contents of this Thesis in full or in parts, have not been submitted to, and will not be submitted by me to, any other Institute or University in India or abroad for the award of any degree or diploma.



Alankar Agarwal
P14BS001

Certificate

This is to certify that the Thesis titled "*Analysis of Lattice Boltzmann Method for Turbulent Flow Simulation on Multi-core GPU Architecture*", submitted by Alankar Agarwal (P14BS001) to the Indian Institute of Technology Jodhpur for the award of the degree of *Doctor of Philosophy*, is a bonafide record of the research work done by him under my supervision. To the best of my knowledge, the contents of this report, in full or in parts, have not been submitted to any other Institute or University for the award of any degree or diploma.



Dr. B. Ravindra
Ph.D. Thesis Supervisor



Dr. Akshay Prakash
Ph.D. Thesis Co-Supervisor

Acknowledgment

It has been an incredible experience while pursuing a doctoral degree at the Indian Institute of Technology Jodhpur (IITJ). I have been fortunate to share this experience with many people and express a few words of thanks and gratitude for them.

First of all, I thank my Ph.D. Thesis Supervisors, *Dr. B. Ravindra*, and *Dr. Akshay Prakash*, for introducing me to the area of lattice Boltzmann Method (LBM) and its applications. In the process, I have learnt about the problems associated with turbulent flow, and fluid-structure interaction. I am grateful to them for their help and patience and for constantly reminding me to be perfect in the little things that I do each day. Also, I am indebted to the Members of the Doctoral Committee, *Dr. Anand Krishnan Plappally*, *Dr. Sudipto Mukhopadhyay*, and *Dr. Gaurav Bhatnagar*, for their enthusiastic and continued guidance during the research work. I thank *Dr. Laltu Chandra* for his valuable reviews to my work during his stay at IIT Jodhpur.

Further, I am thankful to the Director of IIT Jodhpur for providing such excellent facilities and making my stay at the Institute comfortable and fruitful. I would also like to thank the Department of Mechanical Engineering for providing the research facilities. I am also thankful to the faculty members of the department who were always supporting and helping. Also, I would like to thank all the staff members of the department for providing all sorts of support during my research work. I am grateful to the Office of Academics and Office of Student for their continuous help and support. I am also grateful to the Ministry of Education (MoE), India, for providing the necessary funding and support to carry out this research work.

I wish to give my special thanks to my seniors *Dr. Vikas Pratap Singh*, and *Dr. Dharmesh Kumar* for their continuous support, suggestions, and for helping me get through the difficult times through this entire journey. I would like to give my heartfelt thanks and appreciation to my friends *Gurveer Singh*, *Ankit Agarwal*, *Amrik Singh*, *Abhishek Sahu*, *Tushar Shankar Shinde*, *Ram Niwas Verma*, and *Aniket Dilip Monde* for listening to me and sometimes tolerating me over the past few years.

I acknowledge the Indian Institute of Technology Kharagpur (IIT KGP) administration for my pleasant stay during my visit to IIT KGP. I am also thankful to all my friends and lab-mates in the Department of Aerospace Engineering, IIT KGP, *Animesh Bhowmik*, *Chandan Kumar Sidhant*, *Parth Thakar*, *Hardik Bhaosar*, and *Apurva Raj* for all the discussions in the lab, or at tea-points, and for sharing beautiful moments.

At this moment of accomplishment, I thank all my well-wishers who have directly or indirectly contributed to my work. I am grateful to my late grandmother for all her blessings and for all the important lessons she taught me to make the right decisions in life. I owe my deep sense of gratitude to my parents, *Smt. Uma Agarwal* and *Shri Komeswar Dayal Agarwal* for their day-night efforts, their sacrifices for providing me higher education, and for their relentless belief in me. I am highly thankful for the confidence and the inspiration I have received from my sister, *Mrs. Prerana Agarwal*, and my brother, *Mr. Rajat Agarwal*. I acknowledge and express my sincere gratitude to my brother-in-law, *Mr. Arpit Goel*, for being a part of my family and always stand with me during my tough times. I am also thankful to my wife, *Mrs. Dhawal Gupta*, for her unconditional love and trust. In the end, I thank the biggest to *Baba Trivati Nath*, who was always there to listen, to care, and to help me in every situation irrespective of my little knowledge.

Alankar Agarwal
Ph.D. Student

List of Figures

Figure	Title	page
3.1	Lattice structure of (a) D_2Q_9 , (b) D_3Q_{15} , (c) D_3Q_{19} , and (d) D_3Q_{27} discrete velocity models.	16
3.2	Schematic representation of flow in 3D square duct	19
3.3	2D representation of the full way bounce-back method before (left) and after (right) streaming process.	29
3.4	2D representation of the half way bounce-back method	29
3.5	2D representation of the free-slip boundary condition before (left) and after (right) streaming process.	30
3.6	Illustration of immersed boundary method.	31
3.7	Architecture of Tesla GP100.	33
3.8	Streaming Multiprocessor.	33
3.9	Illustration of CUDA programming model in 3D.	34
4.1	Schematic representation of the flow domain.	38
4.2	Flow behavior of instantaneous streamwise velocity for (a) D_3Q_{15} , (b) D_3Q_{19} , and (c) D_3Q_{27} velocity models.	39
4.3	Centerline distribution of mean streamwise velocity (red plus : D_3Q_{15} , green asterisk : D_3Q_{19} , blue open circle : D_3Q_{27} , open triangle : Kim et al. [2004], filled square: Nakagawa et al. [1999]).	40
4.4	Profiles of mean streamwise velocity (red plus : D_3Q_{15} , green asterisk : D_3Q_{19} , blue open circle : D_3Q_{27} , open triangle : Kim et al. [2004], filled square: Nakagawa et al. [1999]) : (a) $x^*/d = 1.0$, (b) $x^*/d = 3.5$, (c) $x^*/d = 6.0$, (d) $x^*/d = 8.5$.	40
4.5	Profiles of mean normal velocity (red plus : D_3Q_{15} , green asterisk : D_3Q_{19} , blue open circle : D_3Q_{27} , open triangle : Kim et al. [2004], filled square: Nakagawa et al. [1999]) : (a) $x^*/d = 1.0$, (b) $x^*/d = 3.5$, (c) $x^*/d = 6.0$, (d) $x^*/d = 8.5$.	41
4.6	Profiles of RMS streamwise velocity fluctuations (red plus : D_3Q_{15} , green asterisk : D_3Q_{19} , blue open circle : D_3Q_{27} , open triangle : Kim et al. [2004], filled square: Nakagawa et al. [1999]) : (a) $x^*/d = 1.0$, (b) $x^*/d = 3.5$, (c) $x^*/d = 6.0$, (d) $x^*/d = 8.5$.	41
4.7	Profiles of RMS normal velocity fluctuations (red plus : D_3Q_{15} , green asterisk : D_3Q_{19} , blue open circle : D_3Q_{27} , open triangle : Kim et al. [2004], filled square: Nakagawa et al. [1999]) : (a) $x^*/d = 1.0$, (b) $x^*/d = 3.5$, (c) $x^*/d = 6.0$, (d) $x^*/d = 8.5$.	42
4.8	Profiles of Reynolds shear stress (red plus : D_3Q_{15} , green asterisk : D_3Q_{19} , blue open circle : D_3Q_{27} , open triangle : Kim et al. [2004], filled square: Nakagawa et al. [1999]) : (a) $x^*/d = 1.0$, (b) $x^*/d = 3.5$, (c) $x^*/d = 6.0$, (d) $x^*/d = 8.5$.	42
4.9	GPU performance of discrete velocity.	44
4.10	Centerline distribution of mean streamwise velocity (asterisk : BB, open circle : IB, open triangle : Kim et al. [2004], filled square : Nakagawa et al. [1999]).	45
4.11	Profiles of mean streamwise velocity (asterisk : BB, open circle : IB, open triangle : Kim et al. [2004], filled square : Nakagawa et al. [1999]) : (a) $x^*/d = 1.0$, (b) $x^*/d = 3.5$, (c) $x^*/d = 6.0$, (d) $x^*/d = 8.5$.	45
4.12	Profiles of mean normal velocity (asterisk : BB, open circle : IB, open triangle : Kim et al. [2004], filled square : Nakagawa et al. [1999]) : (a) $x^*/d = 1.0$, (b) $x^*/d = 3.5$, (c) $x^*/d = 6.0$, (d) $x^*/d = 8.5$.	45

4.13	Profiles of RMS streamwise velocity fluctuations (asterisk : BB, open circle : IB, open triangle : Kim <i>et al.</i> [2004], filled square : Nakagawa <i>et al.</i> [1999]) : (a) $x^*/d = 1.0$, (b) $x^*/d = 3.5$, (c) $x^*/d = 6.0$, (d) $x^*/d = 8.5$.	46
4.14	Profiles of RMS normal velocity fluctuations (asterisk : BB, open circle : IB, open triangle : Kim <i>et al.</i> [2004], filled square : Nakagawa <i>et al.</i> [1999]) : (a) $x^*/d = 1.0$, (b) $x^*/d = 3.5$, (c) $x^*/d = 6.0$, (d) $x^*/d = 8.5$.	46
4.15	Profiles of Reynolds shear stress (asterisk : BB, open circle : IB, open triangle : Kim <i>et al.</i> [2004], filled square : Nakagawa <i>et al.</i> [1999]) : (a) $x^*/d = 1.0$, (b) $x^*/d = 3.5$, (c) $x^*/d = 6.0$, (d) $x^*/d = 8.5$.	46
5.1	Schematic representation of the flow domain	50
5.2	Flow Patterns in the stirred tank reactor with dual-Rushton turbines a) Parallel flow, b) Merging flow, and c) Diverging flow for Case 1, Case 2, and Case 3 respectively in Table 5.1.	52
5.3	Instantaneous velocity magnitude contour at upper impeller location for Case 1: (a) with baffles, (b) without baffles.	52
5.4	Instantaneous velocity magnitude contour at upper impeller location for Case 2: (a) with baffles, (b) without baffles.	53
5.5	Instantaneous velocity magnitude contour at upper impeller location for Case 3: (a) with baffles, (b) without baffles.	53
5.6	Phase-averaged velocity magnitude contour at upper impeller location for Case 1: (a) with baffles, (b) without baffles.	54
5.7	Phase-averaged velocity magnitude contour at upper impeller location for Case 2: (a) with baffles, (b) without baffles.	54
5.8	Phase-averaged velocity magnitude contour at upper impeller location for Case 3: (a) with baffles, (b) without baffles.	55
5.9	Phase-averaged velocity magnitude contour at $\theta = 0^\circ$ for Case 1: (a) with baffles, (b) without baffles.	55
5.10	Phase-averaged velocity magnitude contour at $\theta = 0^\circ$ for Case 2: (a) with baffles, (b) without baffles.	56
5.11	Phase-averaged velocity magnitude contour at $\theta = 0^\circ$ for Case 3: (a) with baffles, (b) without baffles.	57
5.12	Comparison of axial profiles of phase-averaged radial velocity in a plane midway between baffles at different radial locations for Case 1.	57
5.13	Comparison of axial profiles of phase-averaged radial velocity in a plane midway between baffles at different radial locations for Case 2.	58
5.14	Comparison of axial profiles of phase-averaged radial velocity in a plane midway between baffles at different radial locations for Case 3 [Agarwal <i>et al.</i> , 2021].	58
5.15	Comparison of axial profiles of turbulent kinetic energy in a plane midway between baffles at different radial locations for Case 1.	59
5.16	Comparison of axial profiles of turbulent kinetic energy in a plane midway between baffles at different radial locations for Case 2.	59
5.17	Comparison of axial profiles of turbulent kinetic energy in a plane midway between baffles at different radial locations for Case 3	60
B1	Centerline distribution of mean streamwise velocity at different grid size (red plus : $1000 \times 200 \times 200$, green asterisk : $800 \times 200 \times 120$, open triangle : Kim <i>et al.</i> [2004], filled square: Nakagawa <i>et al.</i> [1999]).	73
B2	Profiles of mean streamwise velocity at different grid size (red plus : $1000 \times 200 \times 200$, green asterisk : $800 \times 200 \times 120$, open triangle : Kim <i>et al.</i> [2004], filled square: Nakagawa <i>et al.</i> [1999]) : (a) $x^*/d = 1.0$, (b) $x^*/d = 3.5$, (c) $x^*/d = 6.0$, (d) $x^*/d = 8.5$.	74

B3	Profiles of RMS streamwise velocity fluctuations at different grid size (red plus : $1000 \times 200 \times 200$, green asterisk : $800 \times 200 \times 120$, open triangle : Kim <i>et al.</i> [2004], filled square: Nakagawa <i>et al.</i> [1999]) : (a) $x^*/d = 1.0$, (b) $x^*/d = 3.5$, (c) $x^*/d = 6.0$, (d) $x^*/d = 8.5$.	74
B4	Profiles of Reynolds shear stress at different grid size (red plus : $1000 \times 200 \times 200$, green asterisk : $800 \times 200 \times 120$, open triangle : Kim <i>et al.</i> [2004], filled square: Nakagawa <i>et al.</i> [1999]) : (a) $x^*/d = 1.0$, (b) $x^*/d = 3.5$, (c) $x^*/d = 6.0$, (d) $x^*/d = 8.5$.	74
B5	Comparison of axial profiles of phase-averaged radial velocity at different radial locations for Case 1 at different grid sizes a) with baffles, and b) without baffles.	75

List of Tables

<i>Table</i>	<i>Title</i>	<i>page</i>
3.1	NVIDIA Tesla GP100 specifications	34
4.1	Comparison of drag coefficient	43
4.2	Computational efficiency of discrete velocity models on GPU cluster	44
4.3	Comparison of drag coefficient	47
4.4	Computational efficiency of BB and IB method on GPU cluster	47
5.1	Reactor and impellers dimensions [Rutherford et al., 1996]	50

List of Symbols

Symbol	Description
c	lattice speed
\overline{C}_D	mean drag coefficient
c_s	speed of sound
C_s	Smagorinsky constant
C_1, C_2, C_3	impeller clearance (cm)
d	diameter of square cylinder (mm)
D	impeller diameter (cm)
D_c	circular disk diameter (cm)
D_f	discrete delta function
D_s	shaft diameter (cm)
\vec{e}_k	particle velocity vector in the k^{th} direction
f_k	particle distribution function along direction k
f_k^{eq}	equilibrium distribution function along direction k
f'_k	post-collision states of the particle distribution function along direction k
f''_k	post-forcing particle distribution function along direction k
\overline{f}_k	filtered particle distribution function
\overline{f}_k^{eq}	filtered equilibrium distribution function
F_k	discrete force distribution function along direction k
\vec{F}_b	force vector on the boundary nodes
G	kernel function
H	height of the square duct (mm)
H_w	water level (cm)
k	spatial direction
\mathbf{k}	turbulent kinetic energy (m^2/s^2)
i, j, k	indexing in $x, y,$ and z direction, respectively
L	length of the square duct (mm)
L_{bf}	baffle length (cm)
L_{bl}	blade length (cm)
N	rotational speed of the impeller (rpm)
N_{bf}	number of baffles plate
N_{bl}	number of blades
n	width of mapping window
n_x, n_y, n_z	domain size in x, y, z dimension, respectively
r	radial location (cm)
Re	Reynolds number
\overline{S}	characteristic filtered rate of strain
S_{ij}	filtered strain rate tensor at grid location, i, j
T	diameter of the cylindrical tank (cm)
t_r	simulation run time (sec)
\vec{u}	macroscopic fluid velocity vector (m/s)
u_x, u_y, u_z	magnitude of velocity in $x, y,$ and z direction, respectively (m/s)

Symbol	Description
\vec{U}_b	velocity vector on the lagrangian markers at boundary surface (m/s)
\vec{U}_b^{uf}	unforced velocity vector at boundary nodes (m/s)
$\langle u \rangle$	mean streamwise velocity (m/s)
$\langle v \rangle$	mean normal velocity (m/s)
\vec{u}^{uf}	unforced fluid velocity vector (m/s)
U_m	Mean velocity (m/s)
U_{rad}	radial velocity of fluid flow (m/s)
U_{tip}	tip velocity of impeller blades (m/s)
V_w	water volume (l)
W	width of the square duct (mm)
W_{bf}	baffle width (cm)
W_{bl}	blade width (cm)
w_k	weight factor along direction k
\vec{x}	position vector of Eulerian fluid nodes
\vec{x}_b	position vector of boundary nodes
x^*	streamwise distance from the downstream face of the cylinder (mm)
x	streamwise dimension (mm)
y	cross-stream dimension (mm)
y	spanwise dimension (mm)
Δ	filter width
$\Delta x, \Delta y, \Delta z$	size of the lattice/ grid spacing in x , y , and z directions, respectively
Δt	time-step size
$\bar{\phi}$	spatial dependent uantity
ρ	density of fluid (kg/m^3)
τ	relaxation time parameter
τ_t	total Relaxation time
ν	kinematic viscosity of the fluid (m/s^2)
ν_{SGS}	eddy viscosity (m/s^2)
ν_t	total effective viscosity (m/s^2)
$\bar{\Pi}_{ij}$	non-equilibrium momentum flux tensor at grid location, i, j
$\langle \cdot \rangle$	time-and spanwise-averaging

List of Abbreviation

Abbreviation	Full form
$2 - D$	Two-Dimensional
$3 - D$	Three-Dimensional
$4 - D$	Four-Dimensional
<i>BB</i>	Bounce-Back
<i>BBL</i>	Bounce-Back on the Link
<i>BTE</i>	Boltzmann Transport Equation
<i>CFD</i>	Computational Fluid Dynamics
<i>CPU</i>	Central Processing Unit
<i>CUDA</i>	Compute Unified Device Architecture
D_2Q_7	Two-dimensional lattice structure with seven velocities
D_2Q_9	Two-dimensional lattice structure with nine velocities
D_3Q_{13}	Three-dimensional lattice structure with thirteen velocities
D_3Q_{15}	Three-dimensional lattice structure with fifteen velocities
D_3Q_{19}	Three-dimensional lattice structure with nineteen velocities
D_3Q_{27}	Three-dimensional lattice structure with twenty-seven velocities
D_mQ_n	Lattice structure of m-dimensional and n-directions
<i>DNS</i>	Direct Numerical Simulation
<i>ELBM</i>	Entropic Lattice Boltzmann Method
<i>FCHC</i>	Face-Centered Hyper Cubic
<i>FD</i>	Finite Difference
<i>FE</i>	Finite Element
<i>FV</i>	Finite Volume
<i>FHP</i>	Frisch, Hasslacher, and Pomeau
<i>GPCs</i>	Graphics Processing Cluster
<i>GPUs</i>	Graphics Processing Units
<i>ID</i>	Index
<i>IB</i>	Immersed Boundary
<i>IB - LBM</i>	Immersed Boundary-Lattice Boltzmann Method
<i>LBE</i>	Lattice Boltzmann Equation
<i>LBGK</i>	Lattice Bhatnagar-Gross-Krook
<i>LBM</i>	Lattice Boltzmann Method
<i>LDA</i>	Laser Doppler Anemometry
<i>LDV</i>	Laser Doppler Velocimetry
<i>LES</i>	Large Eddy Simulation
<i>LGCA</i>	Lattice Gas Cellular Automata
<i>MLUPS</i>	Millions Lattice Updates Per Second
<i>MRT</i>	Multi-Relaxation Time
<i>NS</i>	Navier-Stokes
<i>PDEs</i>	Partial Differential Equations
<i>PE's</i>	Processing Elements
<i>PIV</i>	Particle Image Velocimetry
<i>QELBM</i>	Quasi-Equilibrium Lattice Boltzmann Method

<i>RANS</i>	Reynolds-Averaged Navier-Stokes
<i>RMS</i>	Root-Mean-Square
<i>RPM</i>	Revolution Per Minute
<i>SGS</i>	Subgrid-Scale
<i>SG</i>	Sliding Grid
<i>IO</i>	Inner-outer
<i>SIMD</i>	Single Instruction Multiple Data
<i>SM</i>	Sliding Mesh
<i>SMs</i>	Streaming Multiprocessors
<i>SRT</i>	Single-Relaxation Time
<i>SRT – LBM</i>	Single-Relaxation Time-Lattice Boltzmann Method
<i>SST</i>	Shear-Stress-Transport
<i>TPCs</i>	Texture Processing Clusters
<i>TKE</i>	Turbulent Kinetic Energy